ICSV14
Cairns • Australia
9-12 July, 2007

14th International Congress on Sound & Vibration

EXPERIMENTAL VALIDATION OF LINEAR STABILITY ANALYSIS IN PREMIXED COMBUSTORS SUPPORTED BY ACTIVE CONTROL

Mirko R. Bothien, Jonas P. Moeck, Christian Oliver Paschereit

Institute of Fluid Dynamics and Engineering Acoustics
Technical University Berlin
10623 Berlin, Germany

mirko.bothien@tu-berlin.de

Abstract

In this work, linear stability analysis of combustion systems is compared to experimental investigations. To predict the flame-acoustic interaction a network model in its most simple form, solely based on experimental data, is set up in state-space notation. It is assessed if the model is capable to accurately predict the transition from stable to unstable conditions. The transition is achieved by actively tuning the downstream reflection coefficient of the combustor. Furthermore, it is examined if the calculated growth rates match those of the experiments in the linear regime. Excellent agreement between computations from the model and experiments are found with respect to the transition and the frequency of the least stable mode.

1. INTRODUCTION

One of the main issues in gas turbine development is the stability of the combustion process. By the implementation of lean premixed combustion, stringent emissions restrictions could be followed but the combustion process was adversely affected as it became more susceptible to thermoacoustic instabilities. These instabilities arise from the interaction of unsteady heat release and the acoustic field in the engine. If the two mechanisms constructively interfere, high amplitude pressure pulsations occur, which have a detrimental effect on the combustion process [1].

If adequate models for the combustion chamber acoustics and the dynamic flame response are available, the linear stability of a thermoacoustic system can be assessed. A lot of work has been done on modeling the flame-acoustic interaction leading to thermoacoustic instabilities. Lieuwen & Yang [1, 2] and Nicoud et al. [3] recently gave a comprehensive overview of these research activities. However, the predictive capabilities of such stability analyses with respect to real system behavior are generally not clear. This is due to the fact that often only single operating conditions were considered or the models were not verified with experimental data. In this sense, little effort has been made on investigating, if predicted critical parameter values, for which the combustion system switches from stablity to instability, agree with experimental observations. Matveev & Culick [4] studied this transition by varying the heat input to a Rijke tube and compared it to the predictions of their model. Kopitz et al. [5] were able to predict stable and unstable operating points, which they observed in experimental investigations.

In this work, this lack of a comprehensive experimental validation is addressed by continuously varying the downstream reflection coefficient of the combustion chamber. This is accomplished by using an active control scheme, introduced by Bothien et al. [6], which permits the generation of acoustic boundary conditions ranging from fully reflecting to anechoic. In addition to that, an extension of the common procedure, where the stability of an operating point is classified solely based on the presence of high amplitude pressure pulsations and their frequency is given. Generally, the predicted growth rates are only compared to measurements with respect to their sign, which obviously lacks a quantitative component. In contrast to that, in this work, validation of linear stability analysis is conducted by comparing calculated and experimentally determined linear growth rates of unstable modes.

2. EXPERIMENTAL SETUP

Experiments were conducted in an atmospheric combustor test rig. A schematic overview is shown in Fig. 1. The combustor is operated in lean-premixed mode with a swirl-stabilized burner. An electrical preheater can be used to provide higher air inlet temperatures. Several water-cooled microphones up- and downstream of the flame allow for full identification of the plane wave pressure field by means of the multi microphone method [7]. The OH-chemiluminescence in the flame is monitored with a photomultiplier equipped with an optical bandpass filter that is connected to the combustion chamber via a fiber optic cable. Woofers mounted at both ends of the rig provide for acoustic excitation. All components downstream of the burner have water-cooled walls. The speaker casings are additionally purged with air to prevent hot gases from entering. A more detailed description of the test rig can be found in [8].

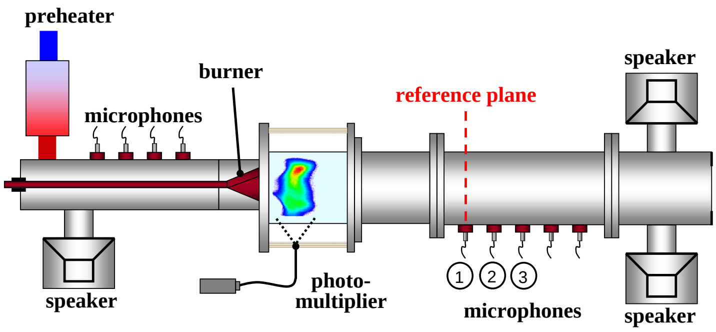

Figure 1. Schematic setup of the atmospheric combustion test rig.

The reference plane drawn in Fig. 1 marks the axial location that is taken as reference for the reflection coefficients. Note here, that this plane is located upstream of the speaker casings. Therefore, the influence of the casings is included in all downstream reflection coefficients shown.

3. ACTIVE CONTROL OF BOUNDARY CONDITIONS

To assess, whether a model is capable to predict the point, at which the combustion system switches from stable to unstable, an appropriate system parameter has to be continuously varied, causing a transition from stability to instability. This could, e.g., either be the burner inlet velocity [9], the equivalence ratio [10], the power [4], the preheat temperature, or the boundary condition. In this work, the downstream reflection coefficient is subject to active change.

Bothien et al. [6] developed an active control scheme, which is able to mimic almost arbitrary outlet impedances. Using this method, the boundary conditions of an acoustic system can be continuously modified ranging from anechoic to fully reflecting. This method was applied in the present study to generate different degrees of reflectivity at the combustor outlet. In this way, a controlled transition from stable to unstable conditions was achieved. The control scheme is shown in Fig. 2. Pressure signals of microphones (labeled 1-3 in Fig. 1) were fed to a control algorithm. The acoustic field (defined by the microphone signals) was decomposed online into its up- and downstream propagating waves g and f, the latter being processed by a suitable control law. A detailed investigation of the decomposition of the acoustic field in time domain is given by Moeck et al. [11].

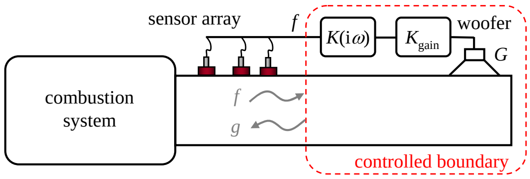

Figure 2. Control scheme for tuning the downstream reflection coefficient.

Based on the reflection coefficient R_{ol} of the uncontrolled system, the one to be adjusted R_{cl}, and the loudspeaker transfer function G, a control law $K(\mathrm{i}\omega)$ was extracted as a function of frequency. To apply it in the control scheme, a model accurately capturing its response was necessary. This model was obtained using frequency domain system identification algorithms.

The controller's output signal drove an acoustic actuator (downstream mounted speakers in Fig. 1), which changed the downstream reflection coefficient to the desired value. In essence, the upstream propagating g-wave (see Fig. 2) is generated by a superposition of the reflected incident f-wave and the wave generated by the actuator.

4. MODELING APPROACH

If entropy waves are neglected and only frequencies below the cut-on frequency for the first non-planar mode are considered, the acoustic state at one location in a ducted geometry is completely defined by two variables. These variables can either be the acoustic pressure p' and velocity u' or the Riemann invariants f and g representing down- and upstream traveling waves, respectively. The primitive acoustic variables are related to the Riemann invariants by $p' = f + g$ and $u' = f - g$, where the acoustic pressure is scaled with the characteristic impedance of the medium.

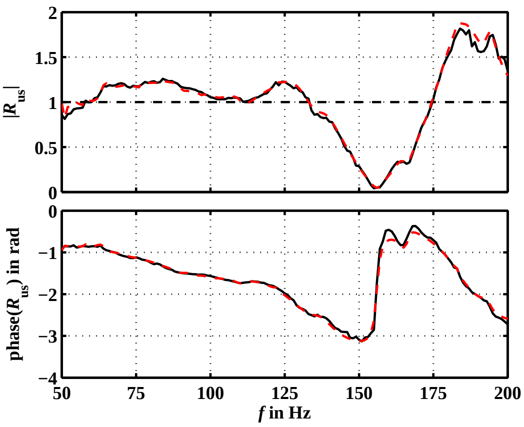

Figure 3. Magnitude and phase of the upstream reflection coefficient R_{us} comprising the flame response (measured: black solid, identified model: red dashed).

The acoustic field in the combustion system was described by the most basic form of a network model. This approach was chosen to minimize modeling uncertainties. The total system was divided into two subsystems, whose thermoacoustic responses were determined experimentally. Through this, the combustor model actually was defined by an up- and downstream reflection coefficient. These reflection coefficients were determined at the position of microphone 1 in Fig. 1. Consequently, the upstream reflection coefficient, denoted R_{us}, comprised the flame response. Measured data for R_{us} are shown in Fig. 3 (solid black). The influence of the flame as an acoustically active element is visible causing a magnitude larger than unity at certain frequencies. R_{us} was measured under stable conditions adjusted by actively reducing the downstream reflectivity (see Sec. 3). Thus, the system was stabilized without changing the flame response, which is crucial as it governs the instability of the system. The downstream reflection coefficient R_{ds} was measured without control.

Determining both reflection coefficients for each operating point experimentally, admits to generate a highly accurate model. Note that the experimental description of a subsystem, however, is not possible in many technical applications. If network elements are determined analytically (e.g., the flame transfer function) or by means of FEM analysis for complex geometries, uncertainties are introduced. Thus, the predictive capabilities of the model are decreased.

Frequency domain system identification tools ([12]) were used to generate state-space representations of the measured reflection coefficients. For the downstream part this state-space model reads

$$\begin{aligned} \dot{x} &= \mathbf{A}x + \mathbf{B}f \\ g &= \mathbf{C}x + Df, \end{aligned} \tag{1}$$

where **A**, **B**, and **C** are time-invariant $N \times N$, $N \times 1$ and $1 \times N$ matrices, respectively and D is a scalar. x is the N-dimensional state vector. Here, the upstream traveling g-wave is obtained from the downstream propagating f-wave. The state-space equations for the upstream end have an analogous form. The identified model is shown in Fig. 3 (red dashed) and shows excellent agreement with the measured R_{us}. Linking together the subsystems' state-space representations results in one single state-space model for the complete system, which is described by $\dot{x} = \mathbf{A}_{\text{con}}x$, where $\mathbf{A}_{\text{con}}$ is the system dynamics matrix. Neither in- nor outputs are present (Fig. 4).

If thermoacoustic stability has to be assessed, modeling systems in state-space has the advantage that for the resulting network system only a matrix eigenvalue problem has to be solved. To assess stability, the temporal evolution of free oscillations has to be considered, which is governed by the dynamics matrix $\mathbf{A}_{\text{con}}$. Similar to the roots of the transcendental dispersion relation in the frequency domain approach, the eigenvalues of the $\mathbf{A}_{\text{con}}$ matrix, s (say), govern the stability of the system. $\Re(s) > 0$ indicates an unstable mode with frequency $|\Im(s)|/2\pi$. This procedure was proposed by Schuermans et al. [13]. Detailed information on setting up low-order network models can be found in [1, 13, 14].

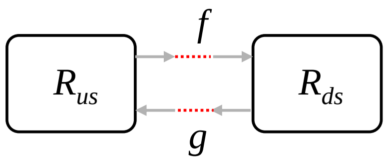

Figure 4. Connection of the two reflection coefficients by means of the Riemann invariants.

5. RESULTS AND DISCUSSION

5.1. Prediction of Stability Border

Using the active control scheme introduced in Sec. 3, the downstream reflection coefficient was continuously reduced in the controlled frequency band ranging from approx. 75 Hz to 95 Hz. This is the frequency interval, in which the combustion system gets unstable at an equivalence ratio of $\phi = 0.7$ and a thermal power of 120 kW. The controller transfer function $K(\mathrm{i}\omega)$ was adjusted to generate an anechoic downstream end, i.e., $R_{cl} = 0$. The downstream reflection coefficient R_{ds}, however, has to be changed continuously from the uncontrolled case towards $R_{cl} = 0$ to find the stability border. Therefore, an additional gain K_{gain} is introduced into the control circuit ranging from 0 to 1 (see Fig. 2), where 0 means that no signal is given to the actuator, i.e., $R_{ds} = R_{ol}$ (no control), and 1 results in $R_{ds} = 0$. Continuously changing this gain results in a continuous change of R_{ds}.

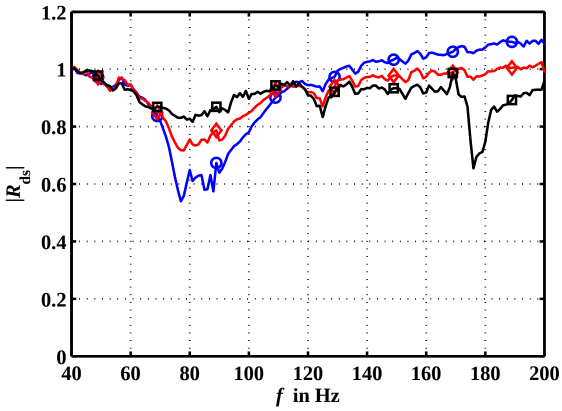

Figure 5. Magnitude of downstream reflection coefficient R_{ds} for different control gains. Black □: $K_{\text{gain}} = 0$ (w/o control), red ◇: $K_{\text{gain}} = 0.15$, blue ○: $K_{\text{gain}} = 0.325$.

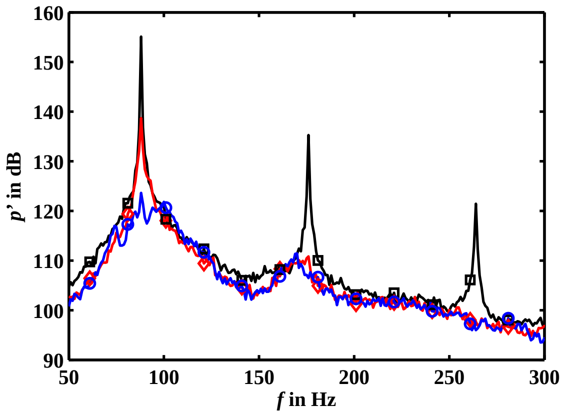

Figure 6. Spectra of the acoustic pressure p' for different control gains. Black □: $K_{\text{gain}} = 0$ (w/o control), red ◇: $K_{\text{gain}} = 0.15$, blue ○: $K_{\text{gain}} = 0.325$.

Figure 5 shows the magnitude of R_{ds} for three different control gains. The uncontrolled case is represented by the black (□) curve, showing that the downstream boundary exhibits strong reflection. The red (◇) and the blue (○) curve show results for a control gain K_{gain} of 0.15 and 0.325. Within the controlled frequency band, R_{ds} was decreased to 0.75 and 0.6, respectively. Above 120 Hz R_{ds} was increased to values larger than unity. This was due to the fact that the controller transfer function was only identified to satisfy the control objective between 75 Hz to 95 Hz. For frequencies outside this interval, the identification algorithm set $K(\mathrm{i}\omega)$ to values, which caused an increase of R_{ds} (see [6]). In Fig. 6, the spectra for these three cases are depicted. Without control (black □) a distinct peak at 88 Hz and its multiples can be seen representing the $\lambda/4$-mode of the test rig. This indicates a strong thermoacoustic instability with a peak amplitude of approximately 156 dB (≈ 1.7 kPa) . Decreasing $|R_{ds}|$ to 0.75 resulted in an attenuation of the peak amplitude of 16 dB. For a downstream reflection coefficient of $|R_{ds}| = 0.6$ the instability was completely suppressed. In this case, the peak amplitude was decreased by 32 dB. According to the results shown, the combustion system switches from unstable to stable somewhere between $R_{ds} = 0.75$ and $R_{ds} = 0.6$.

A phenomenon possibly occurring when changing the operating conditions from unstable to stable is the hysteresis of this transition. In this case, the dynamics of the system depend on the fact, whether the system parameter, which governs stability, is increased or decreased. Hysteretic behavior was, for example, observed when changing the burner exit velocity [9], the equivalence ratio [10], or the power [4]. As the stability analysis is merely valid in the linear regime, it is obvious that if hysteresis occurs, the model can only capture the transition from stable to unstable conditions. Figure 7 proves that hysteresis can be ruled out for the variation of the downstream reflection coefficient. It shows the spectral peak amplitudes of the acoustic pressure and the fluctuation of the OH radical for increasing (black × and blue +)

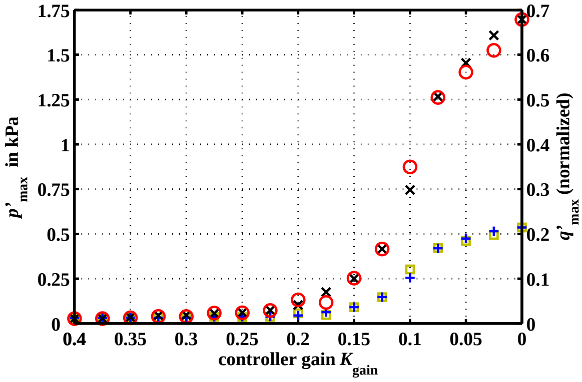

Figure 7. Spectral peak amplitude of acoustic pressure p' and OH fluctuation q' for increasing (black $\times$ and blue $+$) and decreasing (red $\circ$ and yellow $\square$) the control gain K_{gain}.

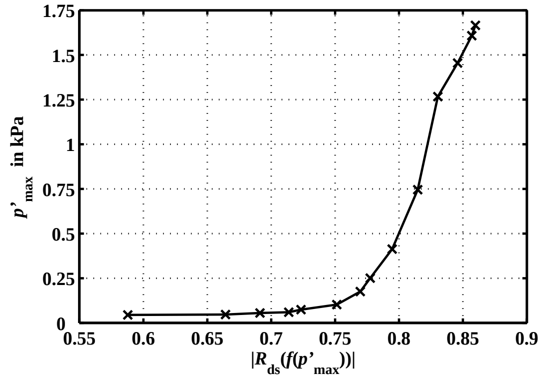

Figure 8. Spectral peak amplitude of acoustic pressure p' as a function of the downstream reflection coefficient $|R_{ds}|$ at the frequency of maximal pressure.

and decreasing (red $\circ$ and yellow $\square$) control gain K_{gain}. Only slight deviations were observed. Each control gain K_{gain} corresponds to a certain controlled downstream reflection. The relation between the downstream reflection coefficient $|R_{ds}|$ and the spectral peak amplitude p'_{max} is shown in Fig. 8. For $|R_{ds}| > 0.8$, p'_{max} rapidly increases, whereas it remains almost constant for $|R_{ds}| < 0.75$. This indicates a transition from stable to unstable behavior.

In the upper frame of Fig. 9, the calculated growth rates $\Re(s)$ for the least stable mode are plotted versus the magnitude of the downstream reflection coefficient $|R_{ds}|$. The red line represents the stability border with a growth rate of 0. As can be seen, the model predicts a transition from stable to unstable at $|R_{ds}| = 0.782$ corresponding to a control gain of 0.1. Decreasing K_{gain}, i.e., increasing $|R_{ds}|$, was computed to have a clearly destabilizing effect as the growth rate increased. For $|R_{ds}| < 0.78$ a negative growth rate was calculated, thus, predicting all modes to be damped.

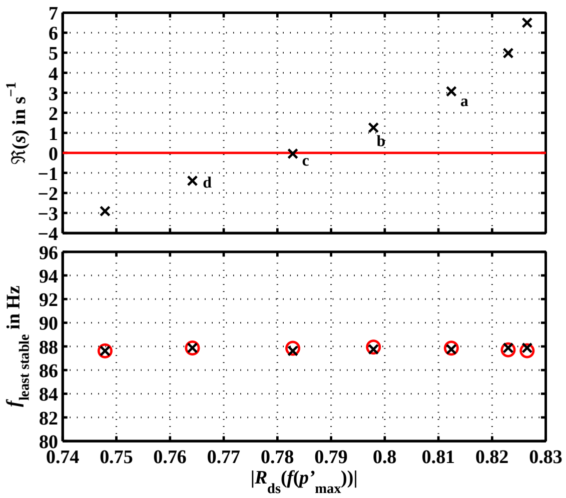

Figure 9. Growth rate $\Re(s)$ (top) and frequency (bottom) of the least stable mode as a function of $|R_{ds}|$.

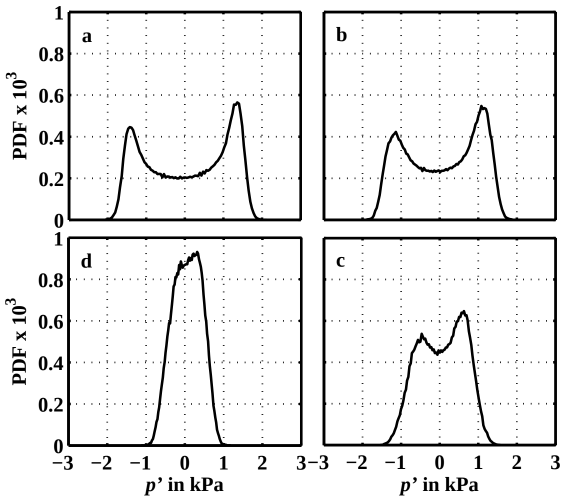

Figure 10. Probability density functions of the acoustic pressure for different $|R_{ds}|$ specified in Fig. 9.

The model results agree with the observations, made in the previous paragraph. However, these observations were purely visual and obviously do not allow to unambiguously decide at which point the combustion system switches from unstable to stable. To assess how accurate the model determines the stability border, the probabilty density functions (PDF) of the pressure fluctuations were calculated. The PDF of a harmonic signal (limit cycle at the instability frequency) superposed by noise, typically shows a clearly bimodal structure. This is due to the reason that the system spends more time near the extremal values of the limit cycle ([9, 15]). Figure 10 shows the PDFs of the points denoted a-d in Fig. 9. Starting from the upper left frame (a), $|R_{ds}|$ is continuously decreased in clockwise direction. Both upper frames (a, b) show cases for a positive growth rate. Peaks at approximately 1.5 kPa and 1.2 kPa indicate strong limit cycle pressure oscillations. At the predicted stability border (c) only small humps at 0.5 kPa were observed, which vanish when $|R_{ds}|$ is further decreased (d). Particularly at the stability border, the combustion process can easily be influenced by little disturbances, which cause the system to switch between stablility and instablility. Hence, this is the reason for the two indistinct extrema in Fig. 10 c. The unsteady pressure distribution in Fig. 10 d typically occurs during stable operation [9]. As stated by Rowley et al. [15], a system is in a limit cycling state, if two distinct peaks are present in the PDF. However, if only a single peak (Fig. 10 d) is observed, it cannot be concluded for sure that the system is not in a limit cycle, as it may be hidden in the noise. Nonetheless, it can be stated that noise is the dominant mechanism and that the model is clearly mature in predicting the operating conditions, which are governed by the limit cycle. To gain further insight, the growth rates were experimentally determined and compared to those obtained from the model. Results are shown in the next section.

Concerning the frequency of the least stable mode, results from the model almost exactly match the experimental observations. This fact is shown in Fig. 9 (bottom), where the measured frequencies ($\circ$) and the computed ones ($\times$) are plotted versus $|R_{ds}|$. The deviation is smaller than 0.3 Hz. It should be mentioned here that the determination of the stability border is sensitive to the accuracy of the system identification. Slight inaccuracies in the model can cause large variations in the computed growth rates. This is in contrast to the determination of the least stable mode's frequency, which is found to be less sensitive to inaccuracies.

5.2. Determination of Growth Rates

For the determination of the linear growth rate $\Re(s)$ the procedure proposed by Moeck et al. [8] was applied. The linear growth rate of the unstable $\lambda/4$-mode was determined from ensemble averaging the transition process from stable to unstable. Unsteady pressure data of a large number of these transition processes could be captured by automatically switching the controller between two different control gains K_{gain} at a frequency of 2 Hz. As there is a range of $|R_{ds}|$, for which the combustion system is unstable (see Sec. 5.1), $\Re(s)$ was determined always starting from the same stabilized state, which was than switched to different $|R_{ds}|$. It was made sure that both, stabilization and growth to limit cycle amplitude, were fully captured.

To obtain the linear growth rate of the unstable mode, an exponentially growing harmonic wave given by

$$x(t) = a_0 \mathrm{e}^{\alpha t} \cos(\omega t + \phi) \tag{2}$$

was identified to each realization of the linear stage of the transition process. Here, a_0, ω, ϕ and α denote initial amplitude, frequency, phase and linear growth rate of the wave and were all subject to the identification process. As the model is only valid in the linear regime, it has to be ensured that only the linear part of the growth rate is determined from the experimental data, i.e., before the process starts to be saturated. The four parameters describing the exponentially growing harmonic wave were found by using a non-linear optimization routine to minimize the error between the analytic expression Eq. (2) and the measured sensor signal in a least squares sense. The parameters governing the growing wave were determined individually for each sensor. In the linear stage of the transition process, all sensor signals grow at the same rate [8]. One realization of the transition process capturing the linear growth of the combustor pressure is shown in Fig. 11.

However, due to a high noise level and slight variations in the mean operating conditions, the measured growth rate deviates from the statistical mean. For this reason, ensemble averages based on a large number of realizations were determined. A histogram of the growth rates of these realizations, comprising the three microphones and the photomultiplier signals, is shown in Fig. 12. The high variance in the distribution of the experimentally determined growth rates underlines the importance of taking ensemble averages of a large number of realizations.

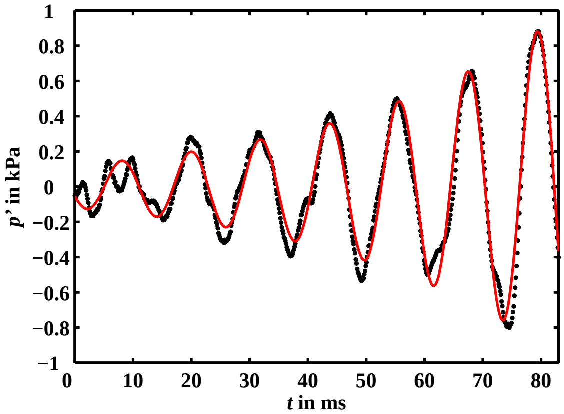

Figure 11. Time traces of acoustic pressure (black dotted) during transition from controlled to uncontrolled state and identified exponential wave (red).

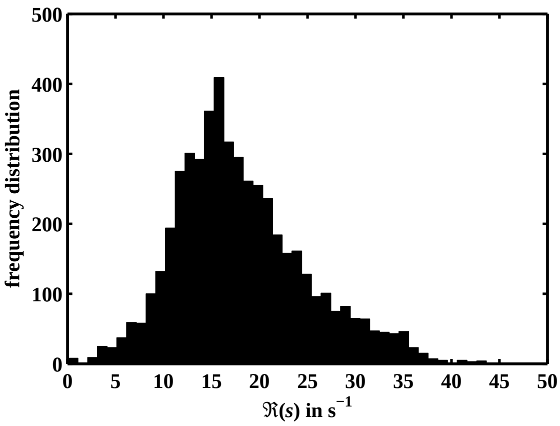

Figure 12. Histogram of linear growth rates $\Re(s)$ from controlled to uncontrolled state calculated with Eq. (2).

Figure 13 depicts the averaged growth rates $\Re(s)$ obtained from the four sensors (red $\circ$) and the predictions from the model (black $\times$). The operating conditions were changed to $\phi = 0.75$ at 130 kW. In both cases, the growth rates show the same ascending trend. However, the computed growth rates differ by a constant offset from the experimentally determined ones. It is assumed that this offset is due to the non-linearity of the downstream reflection coefficient at high pressure amplitudes. This fact was also observed by Heckl [16], who showed that the reflection is reduced by approx. 1% at a sound pressure level (SPL) of 145 dB. As shown in Fig. 6, the SPL is more than 10 dB higher in this investigation, which, therefore, causes a further reduction of R_{ds}. Since the model was based on the downstream reflection coefficient, which was measured at high amplitudes, a lower reflectivity as in the linear case is

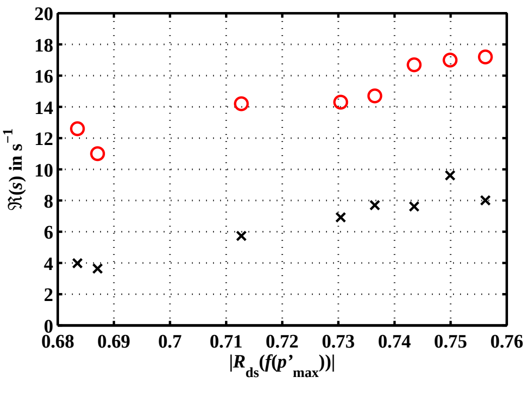

Figure 13. Growth rates $\Re(s)$ in s^{-1} determined from experiments (red $\circ$) and predicted by the model (black $\times$) as a function of the downstream reflection coefficient R_{ds}.

considered in the model. The non-linear effects of R_{ds} are subject to further research.

6. SUMMARY

An experimentally determined model was used to capture the flame-acoustic interaction in a premixed combustor. It was shown that this model was able to accurately reproduce the transition from stability and instability as well as the frequency of the least stable mode. In the experiments, this transition was achieved by actively changing the downstream reflection coefficient. Furthermore, it was investigated, whether the calculated linear growth rates match those of the experiments. Regarding the change of growth rates with changing downstream reflection, the model computed the correct trends. However, a constant offset was observed, presumably caused by non-linear effects of the boundary condition due to high pressure pulsations. Note that if models are used consisting of elements, whose transfer functions are not only determined experimentally, the uncertainties of the predictions will be increased.

REFERENCES

[1] Lieuwen, T. C., and Yang, V., eds., 2005. *Combustion Instabilities in Gas Turbine Engines*, Vol. 210 of *Progress in Astronautics and Aeronautics*. AIAA, Inc.

[2] Lieuwen, T., 2003. “Modeling premixed combustion-acoustic wave interactions: A review”. *Journal of Propulsion and Power,* **19**(5), pp. 765–781.

[3] Nicoud, F., Benoit, L., Sensiau, C., and Poinsot, T., 2007. “Acoustic modes in combustors with complex impedances and multidimensional active flames”. *AIAA Journal,* **45**(2).

[4] Matveev, K., and Culick, F., 2002. “Experimental and mathematical modeling of thermoacustic instabilities in a Rijke tube”. AIAA Paper 2002-1013.

[5] Kopitz, J., Huber, A., Sattelmayer, T., and Polifke, W., 2005. “Thermoacoustic stability analysis of an annular combustion chamber with acoustic low order modeling and validation against experiment”. ASME Paper GT2005-68797.

[6] Bothien, M. R., Moeck, J. P., and Paschereit, C. O., 2007. “Impedance tuning of a premixed combustor using active control”. ASME Paper GT2007-27796.

[7] Paschereit, C. O., Schuermans, B., Polifke, W., and Mattson, O., 2002. “Measurement of transfer matrices and source terms of premixed flames”. *J. of Engineering for Gas Turbines and Power,* **124**, pp. 239–247.

[8] Moeck, J. P., Bothien, M. R., Paschereit, C. O., Gelbert, G., and King, R., 2007. “Two-parameter extremum seeking for control of thermoacoustic instabilities and characterization of linear growth”. AIAA Paper 2007-1416.

[9] Lieuwen, T. C., 2002. “Experimental investigation of limit-cycle oscillations in an unstable gas turbine combustor”. *Journal of Propulsion and Power,* **18**(1), pp. 61–67.

[10] Lepers, J., Krebs, W., Prade, B., Flohr, P., Pollarolo, G., and Ferrante, A., 2005. “Investigation of thermoacoustic stability limits of an annular gas turbine combustor test-rig with and without Helmholtz resonators”. ASME Paper GT2005-68246.

[11] Moeck, J. P., Bothien, M. R., and Paschereit, C. O., 2007. “An active control scheme for tuning acoustic impedances”. AIAA Paper 2007-3540.

[12] Gustavsen, B., and Semlyen, A., 1999. “Rational approximation of frequency domain responses by vector fitting”. *IEEE Transactions on Power Delivery,* **14**(3), pp. 1052–1061.

[13] Schuermans, B., Bellucci, V., and Paschereit, C. O., 2003. “Thermoacoustic modeling and control of multi burner combustion systems”. ASME Paper 2003-GT-38688.

[14] Bothien, M. R., Moeck, J. P., Lacarelle, A., and Paschereit, C. O., 2007. “Time domain modelling and stability analysis of complex thermoacoustic systems”. *Proc. IMechE, Part A, Journal of Power and Energy*. (accepted for publication).

[15] Rowley, C. W., Williams, D. R., Colonius, T., Murray, R. M., and Macmynoski, D. G., 2006. “Linear models for control of cavity flow oscillations”. *Journal of Fluid Mechanics,* **547**, pp. 317–330.

[16] Heckl, M. A., 1990. “Non-linear acoustic effects in the Rijke tube”. *Acustica,* **72**, pp. 63–71.